Sigma J Eng Nat Sci, Vol. 40, No. 1, pp. 95-107, March, 2022

Sigma Journal of Engineering and Natural Sciences
Web page info: https://sigma.yildiz.edu.tr
DOI: 10.14744/sigma.2022.00008

Research Article

Investigation of the machining performance of ferritic ductile cast iron in WEDM using response surface methodology

Kutay AYDIN[1*], Levent UĞUR[1], Salih GÜVERCİN[2], Ferhat GÜL[3]

[1]Department of Mechanical Engineering, Amasya University, Amasya, Turkey
[2]Department of Machinery and Metal Technology, Amasya University, Amasya, Turkey
[3]Department of Metallurgical and Materials Engineering, Gazi University, Ankara, Turkey

ARTICLE INFO

Article history
Received: 09 December 2020
Accepted: 11 March 2021

Key words:
Ductile cast iron; GGG-40, WEDM; Machining performance; Response surface methodology

ABSTRACT

Wire electrical discharge machining (WEDM) technology is a special electrothermal processing method that can precisely production of parts with variable stiffness with sharp edges or production of complex geometric parts which are difficult to produce by traditional manufacturing methods. It has an important place in production sector in terms of low energy consumption. In this study, the relationship between processing parameters on surface quality on the ferritic ductile cast iron (GGG-40) material in WEDM process with molybdenum wire was investigated by Response Surface Methodology (RSM). The aim of this study is to determine the optimum process parameters for low-cost production of GGG-40 material with sharp-edged and complex geometry parts using the WEDM method. In experimental works, surface roughness, and process time were investigated using table feedrate, pulse on time, and pulse space as cutting parameters. The surfaces obtained as a result of the experiments were evaluated in terms of surface quality with Scanning Electron Microscopy (SEM), and surface roughness device. According to the findings, it has been observed that the surface roughness has increased with increasing table feedrate, and pulse on time, and surface roughness decreased with pulse space increasing. Also, it is understood that pulse on time is the most important factor effecting surface quality. It has been found that the process time depends on only the table federate where they are inversely proportional. As result of RSM analysis, optimum cutting parameters were obtained in terms of lowest surface roughness, lowest process time and best time/performance condition on both parameters for ferritic ductile cast iron in WEDM process.

Cite this article as: Aydın K, Ugur L, Guvercin S, Gul F. Investigation of the machining performance of ferritic ductile cast iron in wedm using response surface methodology. Sigma J Eng Nat Sci 2022;40(1):95–107.

***Corresponding author.**
*E-mail address: kutay.aydin@amasya.edu.tr

This paper was recommended for publication in revised form by Regional Editor Fatih Akyol

Published by Yıldız Technical University Press, İstanbul, Turkey

INTRODUCTION

The wire electrical discharge machining (WEDM) is a non-traditional manufacturing method which is preferred basically for mold, and gear production. It is widely used in the manufacturing of parts for the military, aerospace, electronics, jewelry, automotive industry, and surgical components with ferrous and non-ferrous engineering materials [1-4]. This manufacturing process can be successfully used to product electrically conductive materials regardless of their hardness, shape, and toughness [5, 6].

In the WEDM, the material is processed in the form of thermoelectric energy (spark form). The WEDM method is based on the principle of machining by electron arc bombardment with brass or molybdenum alloy wire that proceed without touching the fixed workpiece in the dielectric fluid. For each spark, the ionization, and deionization of the dielectric fluid take place for about 10^{-4} – 10^{-6} seconds [7, 8]. The area around of sparks heats up to 10.000 – 20.000°C, and the dielectric fluid around this area evaporates, and then this causes to increased pressure. In addition, a small amount of workpiece, and electrode material melts, and evaporates, causing small craters to form on the surface. The chip is cooled, and removed from the workpiece by dielectric fluid [8-12]. This process eliminates mechanical stresses, and vibration problems during processing due to the lack of direct contact between the electrode, and the workpiece. In this electrothermal process, the crater size, and microstructure formed on the surface of the material varies with table feedrate, wire speed, pulse on time, pulse space, dielectric fluid pressure etc. parameters [13, 14]. A schematic view of the operation of the WEDM is shown in Fig. 2b.

Ferritic ductile cast iron (GGG-40) is a type of cast iron commonly used in the automotive industry to produce gear, crankshafts, drive axle housing, and differential carrier. GGG-40 has a structure composed of spherical graphite regions as a second phase in the ferrite matrix. Owing to this soft microstructure, it has good castability, and machinability, high toughness, good wear, and heat resistance [15-18]. GGG-40 compared to other cast iron, and steel castings; It has superior properties such as excellent castability, low melting point, heat treatment compatibility, better surface quality, and weight-strength ratio [19-21]. Although the machinability of GGG-40 is good, WEDM, and EDM methods are used for complex geometric parts.

In the existing literature, there are studies on the machining of GGG-40 cast iron, and different materials by WEDM. Özdemir and Özek [16] investigated the effect of discharge voltage, discharge current, and wire speed parameters on surface quality, and cutting speed using a WEDM machine with brass wire on GGG-40 cast iron in their work. They have modeled the results using regression analysis method. Chiang, Chang [15] investigated the changing surface topology, and microstructure using RSM (response surface methodology) of GGG-40 cast iron by EDM (electric discharge machining) method. Tosun, Cogun [14] determined the effect of pulse on time, discharge voltage, wire speed, and dielectric fluid pressure cutting parameters on the surface roughness of AISI 4140 steel using ANOVA (analysis of variance) by WEDM (brass wire) method. Li, Guo [22] studied the effect of discharge energy level on surface roughness, microhardness, and EDS (energy-dispersive X-ray spectroscopy) spectra by machined the Inconel 718 with WEDM (brass wire) method. Tosun, Cogun [23] studied the effect of kerf, and material removal rate using Taguchi, and ANOVA methods on machining AISI 4140 steel with pulse on time, discharge voltage, wire speed, and dielectric fluid pressure cutting parameters by WEDM (brass wire) method. Koklu [24] investigated the effect of the kerf, and surface roughness on Al7 475-T7 351 alloy with machining with pulse on time, table feedrate, and wire speed cutting parameters using the Gray-Based Taguchi method by the WEDM (brass wire). Azam, Jahanzaib [25] has modeled the effect of pulse on time, pulse space, discharge current, and wire speed on the cutting speed on HSLA (high strength low alloy) steel alloy using the ANOVA method with the WEDM (molybdenum wire) process. Azam et al. [26], in their other WEDM study, examined the surface of the material cut by EDS method, and observed the remains of the molybdenum material. As the melting temperature of the molybdenum wire was higher than that of the brass wire, they concluded that molybdenum was not transferred by diffusion to the cutting surface. Goswami, Kumar [27], has examined the effect of pulse on time, pulse space, and peak current cutting parameters on material removal rate, and surface roughness on Nimonic-80A alloy using SEM images, and ANOVA method with WEDM process. As a result, they observed that higher pulse on time, and peak current to caused increased discharge energy in other words stronger arc bombardment, and consequently increased material removal rate, but reduced surface quality. They achieved the best surface quality at the lowest selected pulse on time, and peak current, and highest pulse space value [27].

Wire wear rate, cutting rate, and wire failure frequency, kerf size, and surface quality are the most significant factors in the WEDM process [23, 27]. These factors are affected by the processing parameters. For each material or group of materials, optimization of these parameters is required; Otherwise, surface quality defects, and product errors may occur. In this study, the effects of different cutting parameters (table feedrate, pulse on time, pulse space) on surface roughness, and process time using the WEDM machine with molybdenum wire have been investigated. Molybdenum wire is preferred because; owing to molybdenum wire has a high melting temperature, low thermal expansion coefficient, and chemical stability, the diffusion to the cutting surface is low, does not contaminate the surface, and consequently has an effect of increasing the

surface quality [28, 29]. In addition, since the molybdenum wire has high wear resistance, it is not single-use such as a brass wire, and can be used numbers of times by wrapping it in a drum [25, 26, 30]. For this reason, molybdenum wire is preferred instead of brass wire. As a result, this study contributes to the literature by determining the optimum processing parameters of GGG-40 ferritic ductile cast iron in terms of surface quality and process time with the advantages of molybdenum wire in the WEDM process.

EXPERIMENTAL PROCESS

In experimental work, ferritic ductile cast iron (GGG-40), which is widely used in the industry as workpiece, was used. No heat treatment has been applied to the material. The chemical composition of the material is given in Table 1, and the mechanical properties in Table 2. The micrograph of ferritic ductile cast iron is shown in Fig. 1. When the micrographs are examined, it is seen that the structure of the cast GGG-40 is composed of ferrite, and graphite spheres.

Samples were machined on Hightech DK-7732 CNC WEDM machine. On the machine, 0.18 mm Guangming Molybdenum wire was used as WEDM wire, emulsion of pure water, and WEDM Coolant JR3A Ointment (1/30-40 kg/kg at ratio, JR3A/pure water) was used as dielectric coolant fluid. In machines using molybdenum wire, the wire is wrapped around a drum, used repeatedly, and wire speed is dependent on the revolutions per minute of drum. The wire speed has kept constant, and the drum speed has 1600 rpm. The dielectric fluid circulation pressure has kept at a constant 1 bar level. The samples were machined using

Table 1. Chemical Composition of GGG-40 (DIN) Ferritic Ductile Cast Iron Alloy

Alloy Element	Fe	C	Si	Mn	P	S	Mg
Wt. %	Base	3.40	2.75	0.25	0.04	0.015	0.025

Table 2. Mechanical Properties of GGG-40 (DIN) Ferritic Ductile Cast Iron Alloy

Tensile Strength (N/mm^2)	400
Yield Strength (N/mm^2)	250
Elongation (%)	15
Brinell hardness (BHN)	120–180
Modulus of Elasticity (kN/mm^2)	169

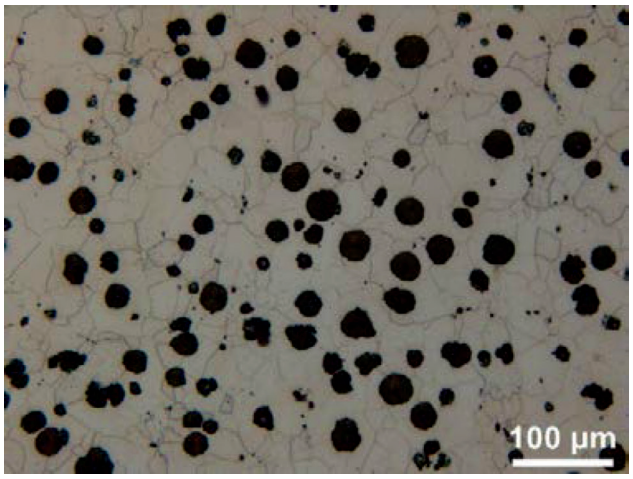

Figure 1. The Micrograph of Ferritic Ductile Cast Iron (GGG-40) x200 Magnification.

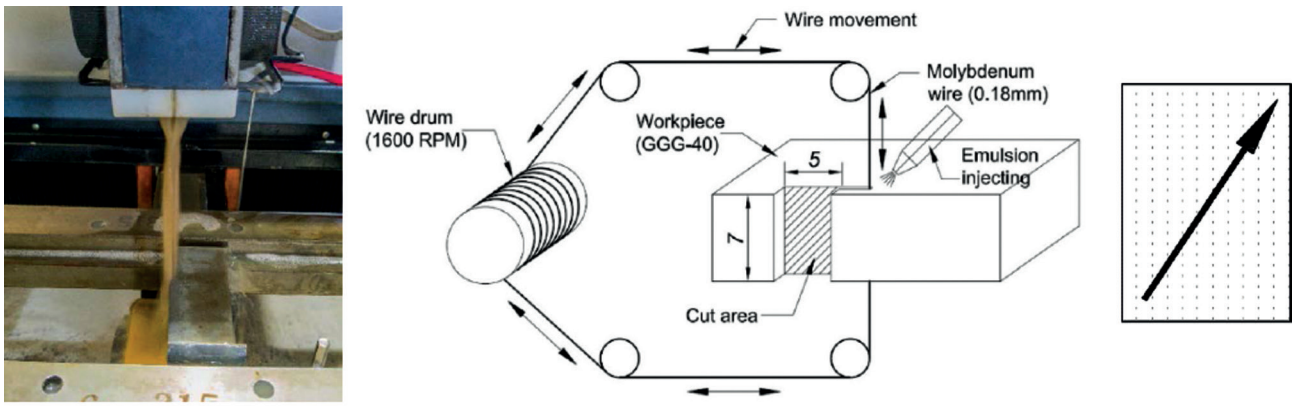

Figure 2. a) Experimental Set Up, **b)** Schematic View of Machining Process, **c)** Surface Roughness Measurement Direction.

different cutting parameters (table feedrate, pulse on time, and pulse space). Cutting parameter levels are shown in Table 3. Cutting parameters were determined with reference to similar studies in the literature [25, 26, 31, 32]. The levels of cutting parameters were selected by conducting pilot experiments.

Experiments were performed in RSM design. The thickness of sample has been selected 7 mm. This thickness has been chosen by considering the feasibility of the experimental parameters, and the applicability of surface roughness measurements. Likewise, the cutting length has been chosen to be 5 mm. The experimental set up, and schematic view of the machining process are shown in Fig. 2a, and 2b. Process times were recorded throughout the experiments. Surface roughness values were measured with Mahr Perthometer M1. The cut-off length (λ_c) of 0.8mm, and traverse length (L_t) of 5.6mm were used in measurements according to ISO 4288. The surface roughness measurement directions on the cutting surfaces are shown in Fig. 2c. For the most consistent measurements, the measurement direction is chosen as the diagonal line of the cutting area.

Table 3. Level of Cutting Parameters

Cutting Parameters	Symbol	Level 1	Level 2	Level 3
		−1	0	+1
Table Feedrate (mm/min)	A	1	2.5	5
Pulse on Time (μs)	B	16	32	64
Pulse Space (μs)	C	4.5	5.25	6

RESPONSE SURFACE METHODOLOGY

Response Surface Methodology (RSM) is a collection of mathematical, and statistical techniques useful for the modelling, and analysis of problems in which a response of interest is influenced by several variables, and the objective is to optimize this response [33–35]. There is a loss in productivity, and quality due to wire breakage. In order to minimize these losses, a comprehensive pilot study should be conducted to select the range of process parameters, and their combination. The RSM is one of the most effective statistical, and mathematical methods that are useful for modelling, and analyze the interactive, and quadratic effects between the variables [36-39]. The main purpose of this technique is to optimize the response surface affected by various processing parameters. RSM has been applied to develop mathematical models in the form of multiple regression equations for the quality features of the WEDM process. The solution of multiple response problems is evaluated in two stages as modeling, and optimization after

Table 4. Design of RSM Matrix and Results

Experiment Run	Process Parameters			Responses	
	A	B	C		
	Table feedrate (mm/min)	Pulse on time (μs)	Pulse space (μs)	Surface Roughness Ra (μm)	Process Time (s/mm²)
E 01	1	-1	0	5.248	1.88
E 02	0	0	0	5.779	3.45
E 03	1	0	-1	6.592	1.77
E 04	-1	-1	0	3.804	8.37
E 05	0	1	1	7.003	3.46
E 06	0	1	-1	7.688	3.42
E 07	1	0	1	6.053	1.64
E 08	0	-1	-1	4.807	3.43
E 09	0	0	0	5.782	3.34
E 10	0	0	0	5.795	3.24
E 11	1	1	0	7.740	1.75
E 12	0	0	0	5.764	3.68
E 13	-1	0	-1	5.626	7.95
E 14	-1	1	0	6.945	7.67
E 15	0	0	0	5.756	3.51
E 16	0	-1	1	4.278	3.42
E 17	-1	0	1	5.074	8.06

data is obtained. When describing the problem, properties that are considered input variables (X_i, $i=1, 2, \ldots, k$), and response variables (Y_j, $j=1, 2, \ldots, r$) were used. In order to develop regression equations related to various quality features of the WEDM process, the second-order response surface is assumed as follows:

$$y = \beta_0 + \sum_{j=1}^{k} \beta_j x_j + \sum_{j=1}^{k} \beta_{jj} x^2_j + \sum_{i}^{k-1} \sum_{j}^{k} \beta_{ij} x_i x_j + \varepsilon \quad (1)$$

In Eq. (1); y response variable, β_0, β_1, β_2,,….β_k unknown regression parameters or regression coefficients; $x_i(i = 1, 2, \ldots, k)$, $x_j(j = 1, 2, \ldots, k)$ input or independent process parameters, and ε is Random error [40].

RESULTS AND DISCUSSION

Experimental Results

Variation of the surface roughness measurements depending on whole cutting parameters are shown in Table 4 for each combination of experiments. Increasing the federate, reduces the interaction time between the wire, and workpiece. This situation causes to increase in surface roughness. As seen in Fig. 3a, the surface roughness is observed to increase by an average of 10% when

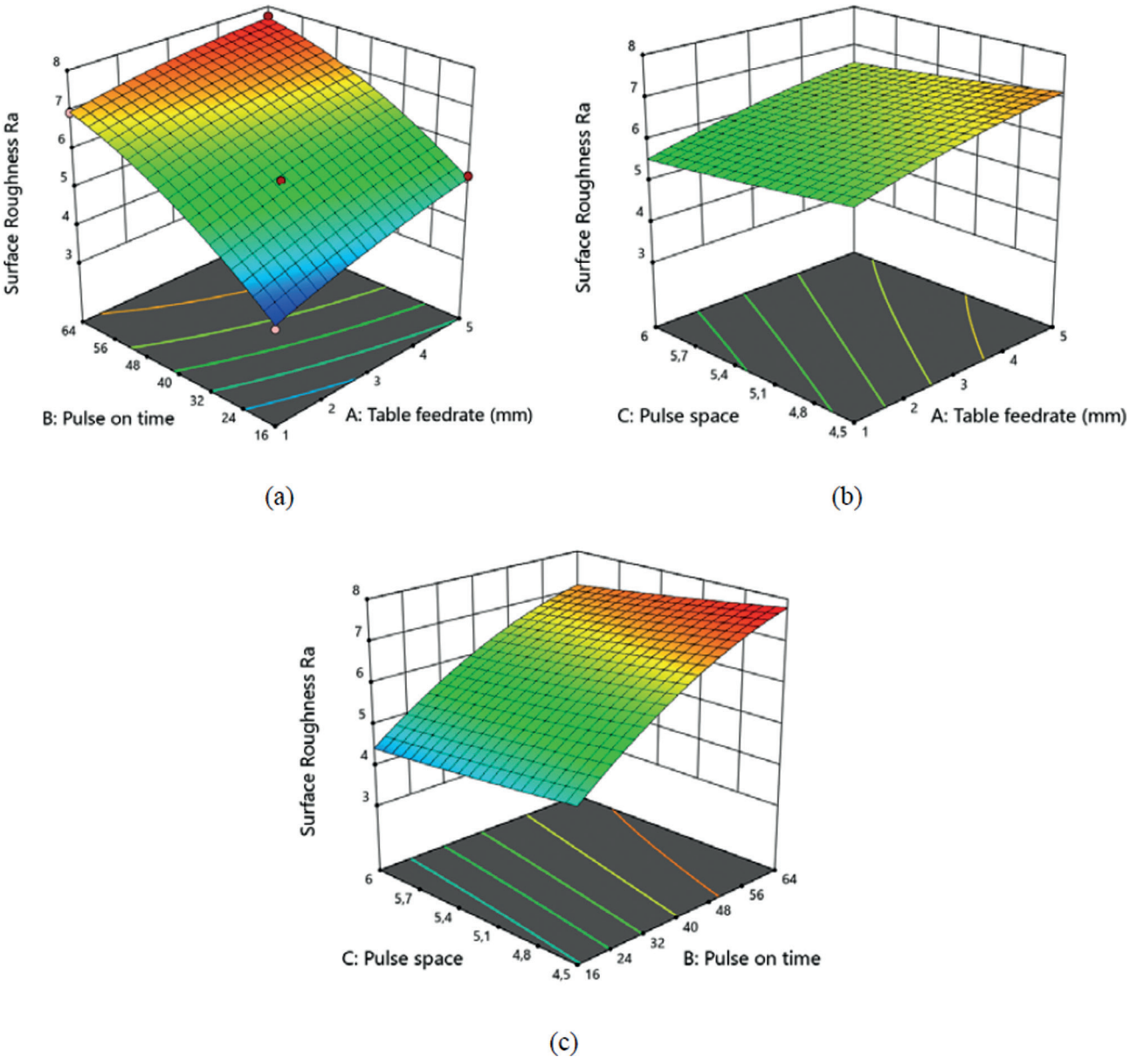

Figure 3. 3D Surface Roughness RSM Graphs According to Process Parameters; **a)** Ra-B-A, **b)** Ra-C-A, **c)** Ra-C-B.

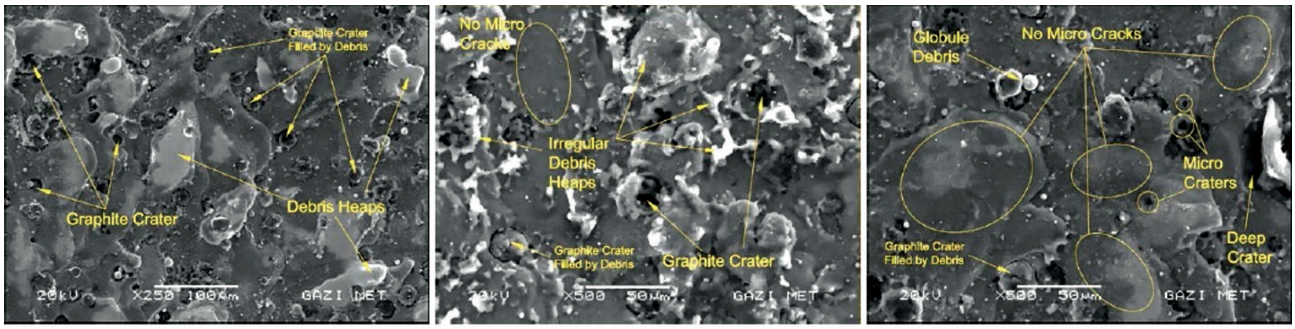

Figure 4. Surface Morphology After WEDM: **a)** E-11 × 250, **b)** E-04 x500, **c)** E-11 × 500.

evaluated all experiment combinations where other cutting parameters are kept constant. The pulse on time is the cutting parameter that determines the duration of the electron bombardment from wire to workpiece. Greater duration of electron bombardment will cause, greater amount of chip removal on workpiece surface, and indirectly greater crater dimensions. This situation also causes to increase in surface roughness [16, 26].

Fig. 3a, 3b and 3c gives (three-dimensional (3D) response surfaces) that the influence of the three different parameters pulse on time, table feedrate and pulse on time on the performance of parameter surface roughness. Fig. 3a shows the interaction plot of pulse on time and table feedrate. As the graph shows, increasing the pulse on time and table feedrate causes increase in the surface roughness. The pulse space is the elapsed waiting time between the electron bombardments (pulse on time) on the workpiece [16, 26]. During this waiting period, the chip is removed from the cutting zone on workpiece with the dielectric fluid. The greater the removal of the chips causes more stable cutting zone, and the less surface roughness [14, 32]. Fig. 3b shows the interaction plot of pulse space and table feedrate. As seen in Fig. 3b, it is understood that the value of Pulse space and table feedrate does not have a significant effect on surface roughness. Fig. 3c shows the interaction plot of pulse space and pulse on time. It can be seen from Fig. 3c that surface roughness decreases when pulse space increases [32]. It is understood from average percent changes in Fig. 3a, 3b and 3c that the cutting parameter, the most effecting parameter for the variation of surface roughness, is the pulse on time.

Cutting Surface Morphology and Contamination

Based on the results seen in Fig. 3; SEM images of the cutting surfaces of the 8th, and 16th experiments (E 08, and E 16) which are the most appropriate, and low-cost in terms of surface quality, and process times, and the 4th, and 11th experiments (E 04, and E 11) with the highest surface quality/lowest process time and highest process time/lowest surface quality were obtained. Fig. 4a, 4b and 4c show x200, and x500 times magnified SEM images of surfaces machined with WEDM. After WEDM process, similar to the studies in the literature, graphite crater filled by debris, regular, and irregular debries, and craters of various sizes were formed on surfaces [26, 27]. The spheroidal graphites shown in Fig. 1 were burned due to the high temperature created by the electric arc during the WEDM and formed graphite craters subsequently. Some of the graphite craters were remaining empty (Fig. 4a, and 4b) but most of them were filled by molten residues during the pulse space. At the same time, micro, and deep crater structures caused by the electric arc are also seen (Fig. 4c). GGG-40 cast iron does not show microcrack formation under high thermal effects due to its ductile, tough, and high thermal resistance structure caused by having high ferrite ratio, and spheroidal graphite [41]. Therefore, no microcrack formation was observed on the cutting surfaces, regardless of the cutting parameters, as shown in Fig. 4b and 4c. During the pulse time, the material surface was eroded, and melted due to the high electric arc, and the resulting high temperature. Immediately after the pulse space phase, these melted materials, and residues formed regular, and irregular debris heaps (Fig. 4a, and 4b).

Fig. 5 show x50, and x100 times magnified SEM images of surfaces machined with WEDM. From these images, the effect of changing the cutting parameters on the surface quality can be understood. Fig. 5a and 5b show the formation of small, and shallow debris on cutting surfaces with the best surface quality. The reason of these are low table feedrate, and short duration arc bombardment. On the contrary, it is seen that larger, deep, and rough debries are formed in Fig. 5c and 5d. From Fig. 5a, 5b, 5c and 5d, it is understood that the increase of table feedrate, and pulse on time caused the surface roughness to increase by creating larger peaks, and pits on the cutting surface.

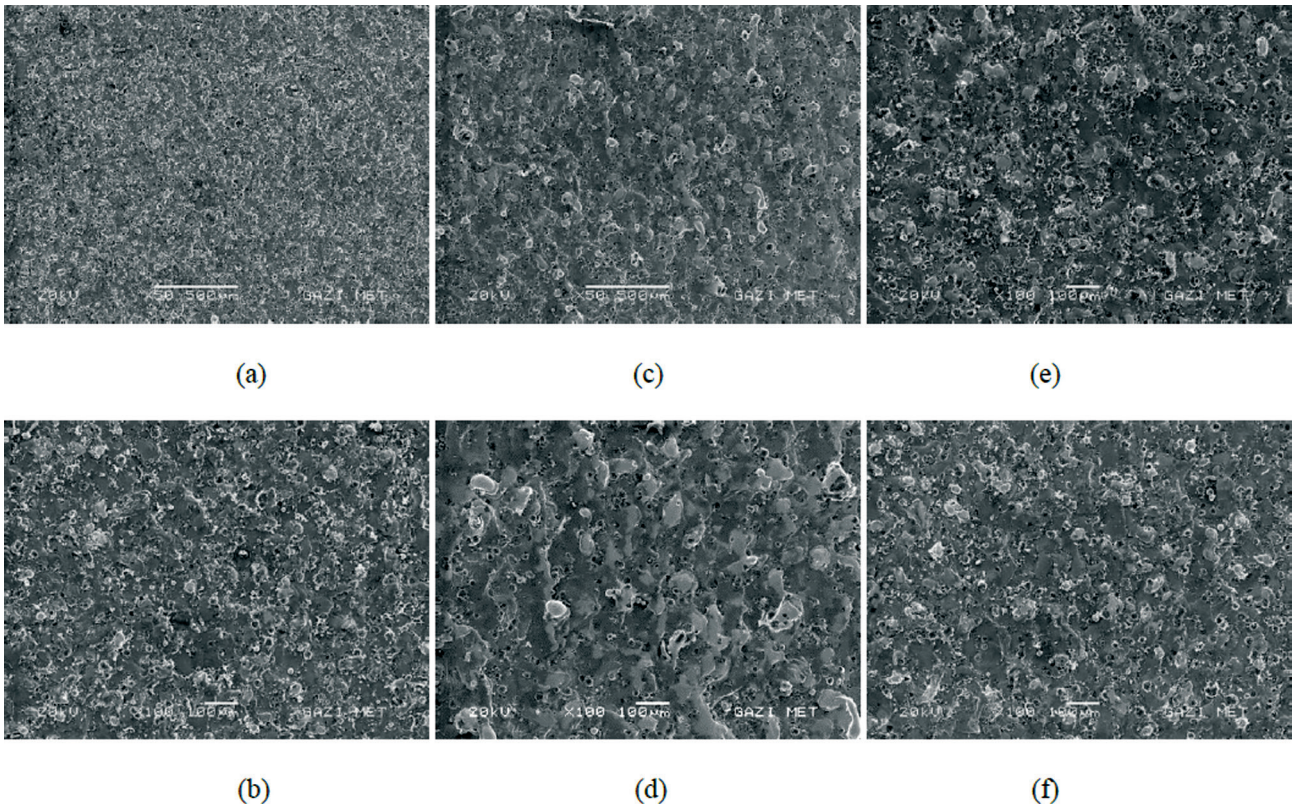

Figure 5. Surface Morphology After WEDM: **a)** E-04 × 50, **b)** E-04 ×100, **c)** E-11 × 50, **d)** E-11 × 100, **e)** E-08 × 100, **f)** E-16 × 100.

Compared to Fig. 5b, 5e and 5f, the similarity of debris sizes are remarkable. From this, it is understood that the surface qualities of these three cutting surfaces are approximately the same. The same pulse on time, different table feedrate, and pulse space values were used in experiment 08, 04, and 16 (Fig. 3). Based on this, it can be said that the pulse on time parameter is the most effective parameter on the surface quality. In experiment 04, and 16 only the table feedrate is different value (Fig. 3). This indicates that the table feedrate effects surface quality less than pulse on time (Fig. 5b, and 5f). In experiment 08, and 16 only the pulse space parameter has changed, and the surface roughness values are very close to each other (Fig. 3). From this, it is understood that the pulse space parameter is the least effective parameter on the surface quality (Fig. 5e and 5f).

Analysis of Surface Roughness

According to a three-level Box-Behnken design combined with response surface methodology. Total 17 experiments were performed and the average values of Surface Roughness Ra (μm) and Process Time (s/mm2) are presented in Table 4. The resulting data needs to be checked for the fists of the models. The model proficiency check includes the importance of the regression model and the lack of fit test. For this purpose, Analysis of Variance (ANOVA) for quadratic model is performed.

The variance analysis according to the surface roughness results of RSM models were shown in Table 5. The model is demonstrated statistically significant due to the fact that the p value is less than 0.05. It also displays the value of R^2-statistic and adjusted R^2-statistic. The R Squared (R^2) is defined as the ratio of the variability described by the model to total variability in actual data. And, this is used as an indicator of goodness of fit. The closer R^2 gets to one, the better the model matches the measured data. The value of R^2 for the model is calculated as 0.9982, shows that 99.82% of the variation for surface roughness is attributed to process parameters and the variation which cannot be explained by the model is 0.18%. This is a definition of the general ability and accuracy of the polynomial model. The predicted R-Squared and adjusted R-squared have close compliance with values 0.9635 and 0.9958 respectively. The ratio of 70.1130 of adequate precision shows an adequate signal.

The empirical relation of RA in terms of actual factors is obtained as follows. The developed second-order for surface roughness (RA) is shown in Eq. (2).

Table 5. ANOVA Table for Surface Roughness

Source	Sum of Squares	df	Mean Square	F-value	p-value	
Model	18.82	9	2.09	408.99	< 0.0001	significant
A-Table feedrate	1.90	1	1.90	372.35	< 0.0001	
B-Pulse on time	14.98	1	14.98	2929.15	< 0.0001	
C-Pulse space	0.6383	1	0.6383	124.86	< 0.0001	
AB	0.0819	1	0.0819	16.02	0.0052	
AC	0.0001	1	0.0001	0.0218	0.8869	
BC	0.0073	1	0.0073	1.43	0.2712	
A^2	0.0450	1	0.0450	8.81	0.0209	
B^2	0.4461	1	0.4461	87.26	< 0.0001	
C^2	0.0037	1	0.0037	0.7243	0.4229	
Residual	0.0358	7	0.0051			
Lack of Fit	0.0348	3	0.0116	49.07	0.0013	significant
Pure Error	0.0009	4	0.0002			
Cor Total	18.85	16				
Std. Dev.	0.0715		R^2	0.998151		
Mean	5.87		Adjusted R^2	0.995774		
C.V. %	1.22		Predicted R^2	0.963489		
			Adeq Precision	70.11301		

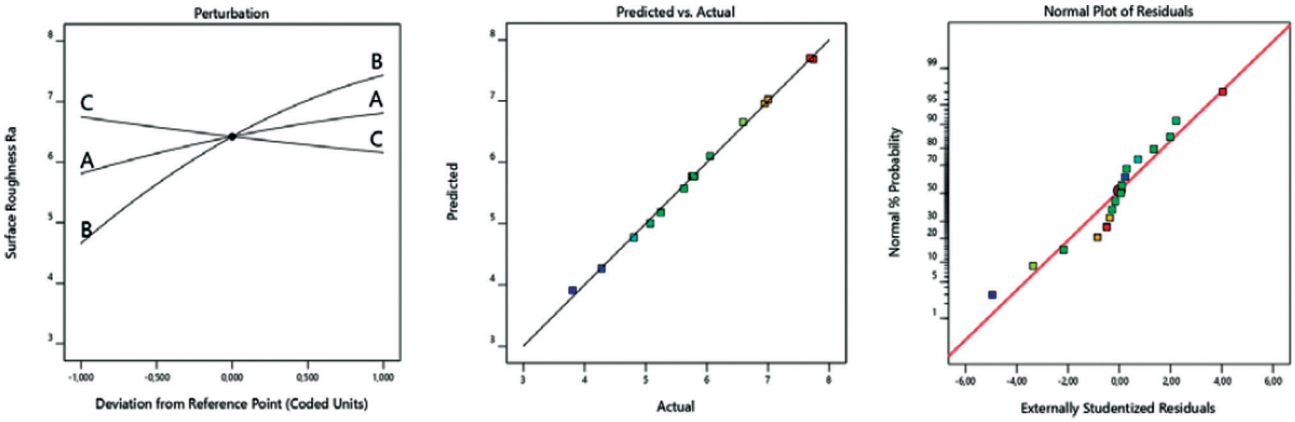

Figure 6. a) Perturbation Plot on Material Removal Rate for GGG-40 Work Piece, **b)** RSM Versus Experimental Predicted Surface Roughness, **c)** Residuals Plot for Surface Roughness.

$$\begin{aligned} Ra = {} & +4.80270 + 0.514399A + 0.130859B \\ & - 0.864557C - 0.002859AB + 0.003465AC \\ & - 0.002311BC - 0.028027A^2 - 0.000654B^2 \\ & + 0.052767C^2 \end{aligned} \quad (2)$$

Comparison of the effect of all the process parameters at the center point on the RA is displayed in the perturbation plot (Fig. 6a). From the response graph, it is observed that the Ra increases with increase in table feedrate and pulse on time whereas Ra decreases by increasing pulse space (Fig. 6a). Residuals plots in Fig. 6b also satisfy the measured values and the predicted values obtained. Straight-line is showed that errors are normally deployed [42, 43]. It is seen

Table 6. ANOVA table for Process time

Source	Sum of Squares	df	Mean Square	F-value	p-value	
Model	87.22	9	9.69	289.14	< 0.0001	significant
A-Table feedrate	73.49	1	73.49	2192.54	< 0.0001	
B-Pulse on time	0.0572	1	0.0572	1.71	0.2326	
C-Pulse space	0.0001	1	0.0001	0.0040	0.9516	
AB	0.0562	1	0.0562	1.68	0.2365	
AC	0.0144	1	0.0144	0.4311	0.5324	
BC	0.0006	1	0.0006	0.0166	0.9012	
A^2	20.26	1	20.26	604.59	< 0.0001	
B^2	0.0138	1	0.0138	0.4108	0.5420	
C^2	0.0044	1	0.0044	0.1305	0.7285	
Residual	0.2346	7	0.0335			
Lack of Fit	0.1221	3	0.0407	1.45	0.3545	not significant
Pure Error	0.1125	4	0.0281			
Cor Total	87.45	16				
Std. Dev.	0.1831		R^2	0.9973		
Mean	4.12		Adjusted R^2	0.9939		
C.V. %	4.44		Predicted R^2	0.9695		
			Adeq Precision	46.8746		

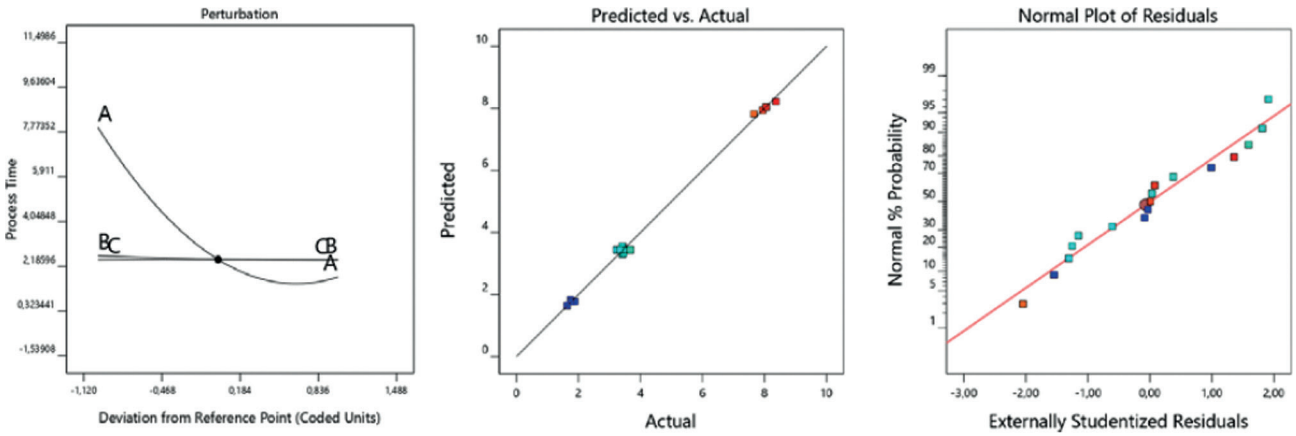

Figure 7. a) Perturbation Plot on Material Removal Rate for GGG-40 Work Piece, **b)** RSM Versus Experimental Predicted Process Time, **c)** Residuals Plot for Process Time.

that the residuals have a normal distribution due to being around a flat line (Fig. 6c).

Analysis of Process Time

Process time is one of the most important parameters in terms of energy saving, and costs. In application, also table feedrate changes as the workpiece thickness changes. As the thickness of the cutting workpiece increases, the wire will try to transfer more electrical arc to the area of workpiece, and at the same time if table feedrate is speed, the wire will strike the workpiece without producing enough electrical arc. For this reason, in application, the table feedrate is selected according to the workpiece thickness. When these are taken into account, the process time is calculated in terms of the time required per unit area (s/mm^2) so that it is independent of the workpiece thickness.

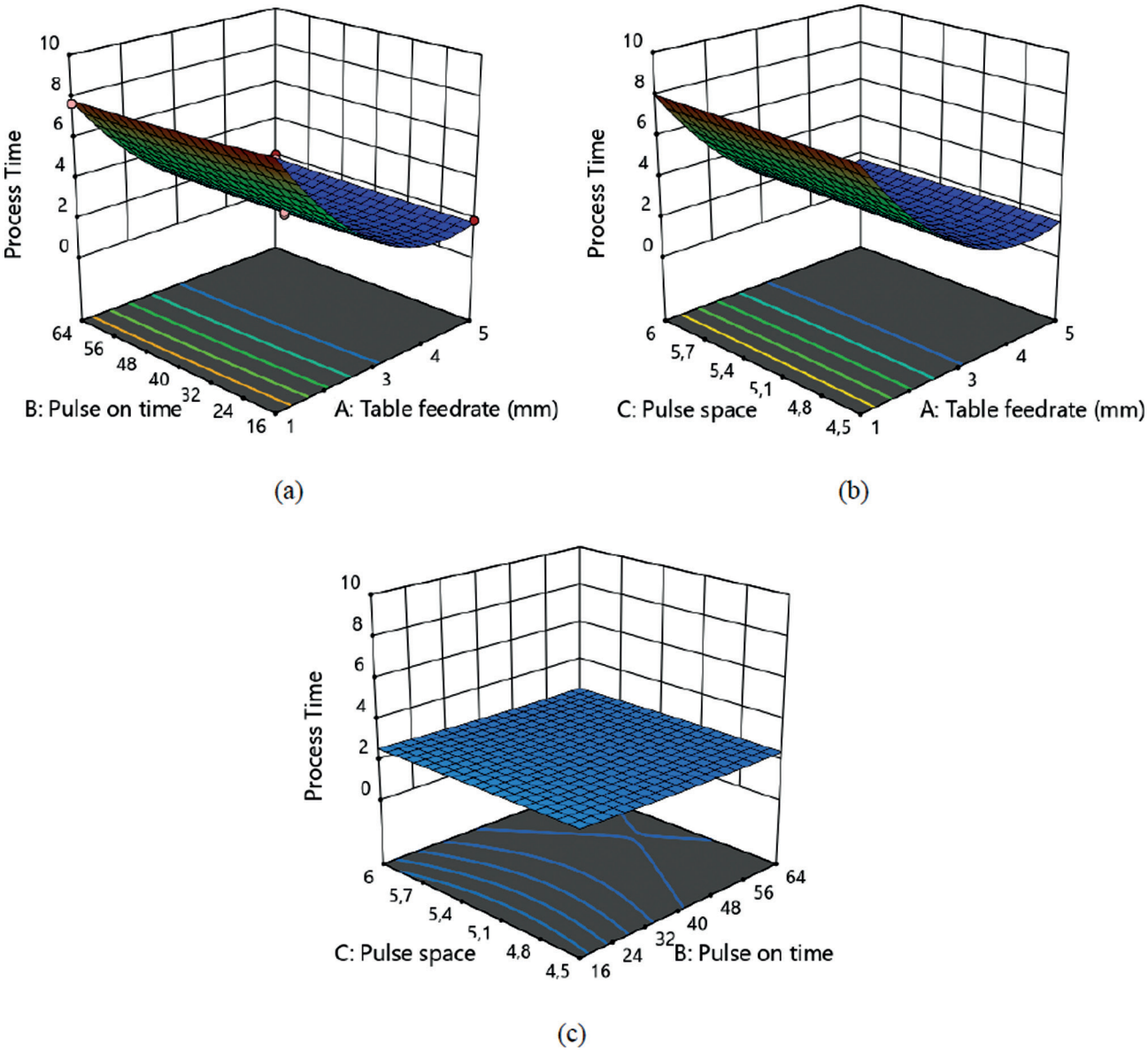

Figure 8. 3D Process Time (Pt) RSM Graphs According to Process Parameters; **a)** Pt-B-A, **b)** Pt-C-A, **c)** Pt-C-B.

The variance analysis according to the process time results of RSM models were shown in Table 6. The model is demonstrated statistically significant due to the fact that the p value is less than 0.05. It also displays the value of R^2-statistic and adjusted R^2-statistic. The R Squared (R^2) is defined as the ratio of the variability described by the model to total variability in actual data. And, this is used as an indicator of goodness of fit. The closer R^2 gets to one, the better the model matches the measured data. The value of R^2 for the model is calculated as 0.9973, shows that 99.73% of the variation for process time is attributed to process parameters and the variation which cannot be explained by the model is 0.27%. This is a definition of the general ability and accuracy of the polynomial model. The predicted R-Squared and adjusted R-squared have close compliance with values 0.9695 and 0.9939 respectively. The ratio of 46.8746 of adequate precision shows an adequate signal.

The empirical relation of Process time in terms of actual factors is obtained as follows. The developed second-order for Process Time (PT) is shown in Eq. (3).

$$\begin{aligned} \boldsymbol{PT} = {} & +11.05677 - 0.500836\boldsymbol{A} - 0.023220\boldsymbol{B} \\ & +0.689559\boldsymbol{C} + 0.002368\boldsymbol{AB} - 0.0039489\boldsymbol{AC} \\ & +0.000638\boldsymbol{BC} + 0.594550\boldsymbol{A}^2 + 0.000115\boldsymbol{B}^2 \\ & -0.057357\boldsymbol{C}^2 \end{aligned} \quad (3)$$

Table 7. Optimization of Response Parameters

Response	Optimize value of input parameters			Predicted value		Experimental value	% error
	A	B	C				
	Table feedrate (mm/min)	Pulse on time (μs)	Pulse space (μs)				
Surface Roughness Ra (μm)	1.15	16.02	5.94	Ra	3.766	3.721	1.209
				Time	7.610	7.55	0.794
Process Time (s/mm²)	4.58	55.40	5.94	Ra	7.145	7.052	1.318
				Time	1.465	1.38	6.159
Surface Roughness and Process Time	3.808	16.00	6.00	Ra	4.676	4.589	1.895
				Time	1.640	1.58	3.797

Comparison of the effect of all the process parameters at the center point on the process time is displayed in the perturbation plot (Fig. 7a). When graph is examined, it can be seen that the increase in the feedrate causes process time to decrease. However, the effect of pulse on time and pulse space changes is not significant on the process time. The relationship between the predicted and the measured values of the process time is shown in Fig. 7b. Straight-line is showed that errors are normally deployed [44, 45]. It is seen that the residuals have a normal distribution due to being around a flat line (Fig. 7c).

Fig. 8a, 8b and 8c gives (three-dimensional (3D) response surfaces) that the influence of the three different parameters pulse on time, table feedrate and pulse on time on the performance of parameter Process time. Fig. 8a shows the interaction plot of pulse on time and table feedrate. When Fig. 8a, 8b and 8c are examined, it is understood that pulse space and pulse on time have no effect on processing time, but increasing the table federate has a powerful effect on process time.

Confirmation Experiments

In this study, three estimation tests were performed for minimum surface roughness, minimum process time and both. Table 7 shows the %error rates between the measured surface roughness values and the RSM results. In line with these results, over 95% agreement was observed between the estimated values and the measured values [46]. %Error rate is calculated as in the following equation:

$$\%error = \left[\frac{(measured\ result - predicted\ result)}{/measured\ result} \right] \times 100 \quad (4)$$

Additional experiments with optimized process parameters not included in the design matrix in Table 4 were conducted to validate the developed model. Actual and estimated values corresponding to the processing parameters selected for the confirmation experiments are shown in Table 7. Error rates between estimated values and actual values are shown in the "% error" column. It has been determined that the estimation % error rates are very low and therefore the estimation performance of the model is quite satisfactory [25, 45]. As a result, it has been understood that the developed model is reliable and can be used for ferritic ductile cast iron (GGG-40).

CONCLUSION

This paper was undertaken experimental work and RSM analysis of machining performance on ferritic ductile cast iron (GGG-40) in WEDM process using different cutting parameters. The following conclusions can be presented:

- WEDM is a sufficient and effective machining method on the processing of GGG-40 for good surface quality and dimensional accuracy.
- Experimental studies have shown that the table feedrate, pulse on time, and pulse space which are selected as cutting parameters, are quite effective on the machining performance of ferritic ductile cast iron (GGG-40).
- It has been understood that the most effective cutting parameter on surface quality is pulse on time. In addition, the cutting parameter, which effecting the process time, was only table feedrate.
- As pulse on time, and table feedrate decreased, and pulse space increased, better surface quality has been obtained.
- Optimized response parameters were obtained from RSM analysis: Table feedrate (A) 1.15 mm/min, pulse on time (B) 16.02 μs and pulse space (C) 5.94 μs should be chosen for the lowest surface roughness. A 4.58 mm/min, B 55.44 μs and C 5.94 μs should be selected for the lowest process time. A 3.80 mm/min,

B 16 µs and C 6 µs should be chosen for optimum surface roughness and process time.
- It is obtained that the most effective parameter is table feedrate in terms of process time.
- The predicted values match the measured values reasonably well, with R2 of 0.9634 for RA and R2 of 0,9695 for process Time.

AUTHORSHIP CONTRIBUTIONS

Authors equally contributed to this work.

DATA AVAILABILITY STATEMENT

The authors confirm that the data that supports the findings of this study are available within the article. Raw data that support the finding of this study are available from the corresponding author, upon reasonable request.

CONFLICT OF INTEREST

The author declared no potential conflicts of interest with respect to the research, authorship, and/or publication of this article.

ETHICS

There are no ethical issues with the publication of this manuscript.

REFERENCES

[1] Ho K. and Newman S. State of the art electrical discharge machining (EDM). Int J Mach Tools Manuf 2003;43:13:1287-1300. [CrossRef]

[2] Nain S.S., Garg D., and Kumar S. Performance evaluation of the WEDM process of aeronautics super alloy. Mater Manuf Processes 2018;33:16:1793-1808. [CrossRef]

[3] Mouralova K, Prokes T, Benes L. Surface and subsurface layers defects analysis after WEDM affecting the subsequent lifetime of produced components. Arab J Sci Eng 2019;44:9:7723-7735. [CrossRef]

[4] Vijayabhaskar S. and Rajmohan T. Experimental investigation and optimization of machining parameters in WEDM of nano-SiC particles reinforced magnesium matrix composites. Silicon 2019;11:4:1701-1716. [CrossRef]

[5] Kansal H, Singh S, Kumar P. Technology and research developments in powder mixed electric discharge machining (PMEDM). J Mater Process Technol 2007;184:32-41. [CrossRef]

[6] Ramasawmy H, Blunt L. Effect of EDM process parameters on 3D surface topography. J Mater Process Technol 2004;148:2:155-164. [CrossRef]

[7] Luis C, Puertas I, Villa G. Material removal rate and electrode wear study on the EDM of silicon carbide. J Mater Process Technol 2005;164:889-896. [CrossRef]

[8] Mouralova K, Kovar J, Klakurkova L, Prokes T, Horynova M. Comparison of morphology and topography of surfaces of WEDM machined structural materials. Measurement 2017;104:12-20. [CrossRef]

[9] Knight WA, Boothroyd G. Fundamentals of metal machining and machine tools. Boca Raton, Florida: CRC Press, 2005.

[10] Tai T, Lu S. Improving the fatigue life of electro-discharge-machined SDK11 tool steel via the suppression of surface cracks. Int J Fatigue 2009;31:3:433-438. [CrossRef]

[11] Snoeys R., Staelens F., and Dekeyser W. Current trends in non-conventional material removal processes. CIRP Ann Manuf Technol 1986;35:2:467-480. [CrossRef]

[12] Esme U, Kulekci MK, Akkurt A, Seker U, Ozkul I. Mathematical modeling of diameter and circularity deviation in wire electrical discharge machining of a hot work tool steel. Mater Test 2013;55:6:472-477. [CrossRef]

[13] Liao Y, Woo J. The effects of machining settings on the behavior of pulse trains in the WEDM process. J Mater Process Technol 1997;71:3:433-439. [CrossRef]

[14] Tosun N, Cogun C, Inan A. The effect of cutting parameters on workpiece surface roughness in wire EDM. Mach Sci Technol 2003;7:2:209-219. [CrossRef]

[15] Chiang K-T, Chang F-P, Tsai D-C. Modeling and analysis of the rapidly resolidified layer of SG cast iron in the EDM process through the response surface methodology. J Mater Process Technol 2007;182:525-533. [CrossRef]

[16] Özdemir N, Özek C. An investigation on machinability of nodular cast iron by WEDM. Int J Adv Manuf Technol 2006;28:869. [CrossRef]

[17] Öztürk B. Experimental research of energy consumption of austenitizing heat-treated casting fittings in pipe threading. Sakarya Üniversitesi Fen Bilimleri Enstitüsü Dergisi 2019;23:5:869-878. [CrossRef]

[18] Voina I-D, Sattel S, Contiu G, Faur A, Luca B. Reamers cutting edge preparation for improvement the GGG 40 machining, MATEC Web of Conferences. EDP Sciences, 2018. [CrossRef]

[19] Kalpakjian S, Vijai Sekar K, Schmid SR. Manufacturing Engineering and Technology. London: Pearson, 2014.

[20] Kacal A, Gulesin M, Melek F. Evaluation of cutting forces and surface roughness at finish turning of GGG 40 ductile iron. J Polytechnic 2008;11:3:229-234.

[21] Nas E, Öztürk B. Optimization of surface roughness via the Taguchi method and investigation of energy

consumption when milling spheroidal graphite cast iron materials. Mater Test 2018;60:5:519-525. [CrossRef]

[22] Li L, Guo Y, Wei X, Li W. Surface integrity characteristics in wire-EDM of Inconel 718 at different discharge energy. Procedia CIRP 2013;6:220-225. [CrossRef]

[23] Tosun N, Cogun C, Tosun G. A study on kerf and material removal rate in wire electrical discharge machining based on Taguchi method. J Mater Process Technol 2004;152:316-322. [CrossRef]

[24] Koklu U. Optimization of kerf and surface roughness of AL 7 475-T 7 351 alloy machined with WEDM process using the grey-based taguchi method. Metalurgija/Metallurgy 2012;51:1:47-50. [CrossRef]

[25] Azam M., Jahanzaib M., Abbasi J.A., and Wasim A. Modeling of cutting speed (CS) for HSLA steel in wire electrical discharge machining (WEDM) using moly wire. J Chin Inst Eng 2016;39:7:802-808. [CrossRef]

[26] Azam M, Jahanzaib M, Abbasi JA, Abbas M, Wasim A, Hussain S. Parametric analysis of recast layer formation in wire-cut EDM of HSLA steel. Int J Adv Manuf Technol 2016;87:713-722. [CrossRef]

[27] Goswami A, Kumar J. Optimization in wire-cut EDM of Nimonic-80A using Taguchi's approach and utility concept. Eng Sci Technol an Int J 2014;17:4:236-246. [CrossRef]

[28] Gajjar DH, Desai JV. Optimization of MRR, Surface roughness and KERF width in wire EDM using molybdenum wire. Int J Res Educ 2015;4:9-17.

[29] Saini H, Khan I, Kumar S, Kumar S. Optimization of material removal rate of WEDM process on mild steel using molybdenum wire. Int J Adv Eng Manag Sci 2017;3:10:239928. [CrossRef]

[30] Newton TR, Melkote SN, Watkins TR, Trejo RM, Reister L. Investigation of the effect of process parameters on the formation and characteristics of recast layer in wire-EDM of Inconel 718. Mater Sci Eng A 2009;513:208-215. [CrossRef]

[31] Ram MS, Varma BS. Investigation of characteristics in electrical discharge machining of certain cast irons using response surface methodology. Int J Appl Eng Res 2017;12:7011-7018.

[32] Sharma N, Khanna R, Gupta R. Multi quality characteristics of WEDM process parameters with RSM. Proced Eng 2013;64:710-719. [CrossRef]

[33] Montgomery D. Design and Analysis of Experiments. 6th ed. New York, NY: John Wiley and Sons, 2005.

[34] Ozturk B. Investigation of effects of inverter frequency changes on the specific energy consumption of pipe threading using response surface methodology. Measurement 2020;152:107296. [CrossRef]

[35] Huang M-L, Hung Y-H, Yang Z-S. Validation of a method using Taguchi, response surface, neural network, and genetic algorithm. Measurement 2016;94:284-294. [CrossRef]

[36] Güvercin S. and Yildiz A. Optimization of cutting parameters using the response surface method. Sigma J Eng Nat Sci 2018;36:113-121.

[37] Şahinoğlu A, Güllü A, Ciftci I. Analysis of surface roughness, sound level, vibration and current when machining AISI 1040 steel. Sigma J Eng Nat Sci 2019;37:423-437.

[38] Belibağlı P, Çiftci BN, Uysal Y. Chromium (Cr (VI)) removal from water with bentonite-magnetite nanocomposite using response surface methodology (RSM). Sigma J Eng Nat Sci 2020;38:1217-1233.

[39] Nnanwube IA, Udeaja JN, Onukwuli OD. Modeling and optimization of zinc recovery from enyigba sphalerite in a binary solution of acetic acid and hydrogen peroxide. Sigma J Eng Nat Sci 2020;38:589-601. [CrossRef]

[40] Montgomery DC. Design and Analysis of Experiments. 4th ed. New York: John Wiley and Sons Inc., 1997.

[41] Faisal M, El-Shenawy E, Taha MA. Thermomechanical testing of GGG 40 spheroidal graphite cast iron alloy. Mater Sci Appl 2017;8:3:273. [CrossRef]

[42] Kaçal A, Yıldırım F. PMD23 Çeliğinin Tornalanmasında CBN Kesici Uçların Kesme Performansının Yüzey Pürüzlülüğü ve Takım Aşınması Üzerindeki Etkilerinin Belirlenmesi. Gazi Üniversitesi Mühendislik Mimarlık Fakültesi Dergisi. 2016;31:181-189. [CrossRef]

[43] Asiltürk I, Neşeli S, Ince MA. Optimisation of parameters affecting surface roughness of Co28Cr6Mo medical material during CNC lathe machining by using the Taguchi and RSM methods. Measurement 2016;78-128. [CrossRef]

[44] Basmacı G, Kırbaş İ, Ay M, Peker M. Karma Taguchi ve yüzey yanıt yöntemi kullanılarak astm b574 (hastelloy c-22)'in tornalanması esnasındaki işleme parametrelerinin yüzey pürüzlülüğüne etkisinin incelenmesi ve kesme parametrelerinin optimizasyonu. Sakarya Univ J Sci 2018;22:2:761-771.

[45] Bayraktar Ş, Hekimoğlu AP. Optimization of thrust force and surface roughness using response surface methodology (RSM) in drilling of Al-30Zn alloy. Gümüşhane Üniversitesi Fen Bilimleri Enstitüsü Derg 2020;10:804-813.

[46] Sarkar S, Mitra S, Bhattacharyya B. Parametric analysis and optimization of wire electrical discharge machining of γ-titanium aluminide alloy. J Mater Process Technol 2005;159:3:286-294. [CrossRef]